Laser-rf double-resonance spectroscopy in the samarium I spectrum: Hyperfine structures and isotope shifts

W. J. Childs, O. Poulsen,* and L. S. Goodman
Argonne National Laboratory, Argonne, Illinois 60439
(Received 19 June 1978)

High-resolution laser-rf double-resonance spectroscopy has been performed in the $4f^6 6s\,^2{}^7F_6$ (4020.66 cm^{-1}), $4f^6 5d6s\,^9H_2$(11044.90 cm^{-1}), $4f^6 5d6s\,^9H_3$ (11406.50 cm^{-1}), and $4f^6 5d6s\,^7H_3$ (13542.80 cm^{-1}) metastable levels of Samarium I. Hyperfine parameters have been deduced with an absolute accuracy of ~ 2 kHz. By means of laser-induced fluorescence, hyperfine constants have been determined in excited levels up to ~ 30560 cm^{-1}, and isotope shifts measured for 11 lines.

I. INTRODUCTION

The spectrum of SmI has been intensively studied using classical spectroscopy, the main reason being the interesting isotope shifts (IS). Striganov *et al.*[1] studied many levels in the even isotopes, showing specific-mass shift contributions, as analyzed by King.[2] This initial work has been followed by several other experimental studies[3,4] that obtained still higher resolution, the Doppler-free laser–atomic-beam technique of Brand *et al.*[4] being a recent example thereof. Theoretically, Bauche *et al.*[5] have analyzed the IS in the ^7F_J ground multiplet. The hyperfine structure (hfs) of this ^7F_J ground term has been determined[6] in atomic-beam magnetic resonance experiments by Woodgate, by Robertson *et al.*, and by Childs and Goodman, with very high precision.

The classification of energy levels has been performed by Blaise *et al.*,[7] thus establishing to a precision of 0.02 cm^{-1} the energy of several hundred levels below $\sim$ 35 000 cm^{-1}.

In this work we report high-resolution measurements of hfs in highly excited, metastable, even-parity states in SmI using the laser-rf double-resonance technique on atoms of a SmI atomic beam. We also report hfs results for odd-parity states up to ~30, 500 cm^{-1} in excitation energy, obtained with sub-Doppler resolution. Finally, precise IS values have been obtained for several SmI lines.

II. TECHNIQUE

The hyperfine structure (hfs) and isotope shift (IS) data have been obtained using a combination of (i) laser-induced fluorescence and (ii) a laser-rf double-resonance technique.

(i) *Laser-induced fluorescence:* High-resolution spectra were obtained by scattering the light from a cw tunable dye laser from a metastable samarium atomic beam, collimated to yield a Doppler width less than 2 MHz. The dye-laser spectral width was ~ 2 MHz thus giving a minimum frequency resolution of ~3–4 MHz. Hence, the fundamental limit in the present experiment is the natural radiation width for lifetimes shorter than ~ 50 ns.

(ii) *Laser-rf double-resonance spectroscopy:* In order to obtain high quality hfs measurements in the discharge-populated, metastable, even-parity Sm I levels, the laser-rf double-resonance technique was applied. This technique is analogous to the classical Rabi magnetic-resonance scheme, but with (monocromatic) laser–atomic-beam interaction regions replacing the inhomogeneons magnetic deflecting fields, as shown in Fig. 1(a). This technique was first used by Rosner *et al.*[8] on a single molecular vibration-rotation level in Na_2. Also Ertmer and Hofer[9] have applied the technique to study atomic hfs in scandium. Recently Rosner *et al.*[10] applied this double-resonance technique to his in singly ionized Xe, thus further demonstrating the potential of the method. The basic scheme in this technique is to empty a particular initial hfs level $\alpha SLJF$ by burning a population hole in its Doppler profile by laser pumping (at the optical frequency ν) to an upper level $\alpha' S' L' J' F'$, as shown in Fig. 1(b). When this upper level mainly decays back to the initial multiplet, the optical pumping (with laser power ~ 5 W/cm^2) typically produces a 20%–50% depletion of the $\alpha SLJF$ level. For discharge-populated, highly excited initial levels the main emission channel is often through decay to different lower multiplets, thus making possible almost complete depletion of a particular hfs level in the initial state even at relatively low laser power. If one now probes the atoms further along their trajectory with light of the same frequency ν, the fluorescence observed will be very weak because of the very small population remaining in the state $\alpha SLJF$.. With a 100% deple-

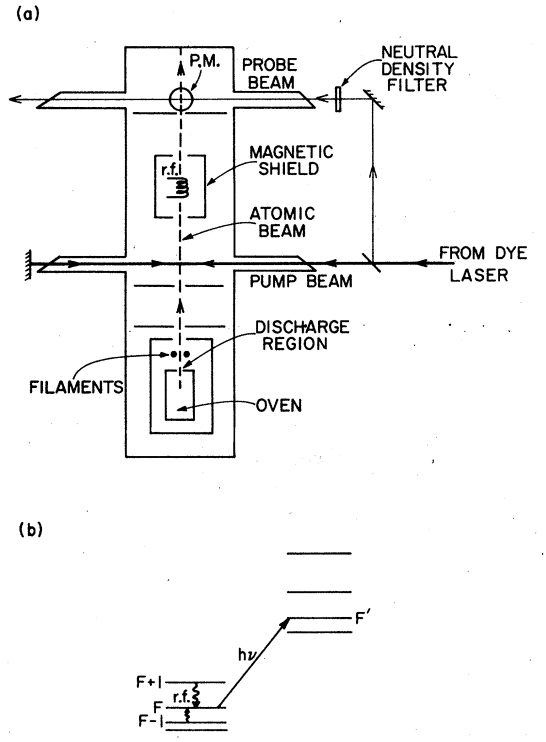

FIG. 1. Experimental setup showing (a) oven section with discharge to populate metastable levels, the laser-pump region, rf section, and finally laser-probe region with PMT to detect the laser-induced fluorescence. (b) Shows the basic scheme in laser-rf double resonance with the pump laser depopulating F; and the rf, when tuned to resonance, repopulating F by inducing rf transitions $\Delta F = \pm 1$, resulting in increased fluorescence in the proble-laser region.

tion, no fluorescence would be detected at all. If, however, a radio-frequency transition is induced between $\alpha SLJF \leftrightarrow F \pm 1$ ($\Delta F = \pm 1$) in the region between the two laser fields (pump and probe) the rf transition repopulates the $\alpha SLJF$ hfs level and an increase in induced fluorescence will result in the laser probe region [Fig. 1(a)]. This effect is resonant in both the laser and rf fields, with the observed rf linewidth determined only by the transit time of the atoms through the rf region and by residual Zeeman splitting. The widths of the rf signals are independent of laser linewidth and laser power shifts, since the rf transitions are induced in the region between the pump and probe laser fields. Typically, widths full width at half-maximum (FWHM) of 15 KHz were obtained. Aside from the requirement that the laser pump beam produce a usable population depletion of the hyperfine substate of interest, the only limit on this technique is that the atomic state must live long enough to traverse the apparatus, the lower lifetime limit being around 0.5 ms for a compact atomic-beam apparatus. One may even have the pump, probe, and rf field regions coincide physically, as shown by Dubke *et al.*[11] in their measurements of the ^{95,97}Mo quadrupole moments, although possible shifts of the rf resonance frequency due to the laser field must be taken into account with this arrangement.

III. APPARATUS

The experimental setup [Fig. 1(a)] consists of a conventional atomic-beam apparatus with an oven section, provision for two laser–atomic-beam interaction regions (pump and probe), a rf section between the two laser interactions, and a Peltier-cooled PMT to monitor the laser-induced fluorescence from the probe-laser interaction. In order to sustain a discharge into the orifice of the Ta oven, the cathodes were placed almost directly over the oven orifice. Initially, heat was produced by electron bombardment. With a sufficiently dense Sm beam effusing from the oven, a discharge was easily initiated. Very stable metastable-state populations and oven-temperature conditions were obtained for discharge conditions of 50 V and 300 mA.

The rf region is shielded from the earth's magnetic field by an outer soft iron shield and an inner heat-treated hypernom shield; the actual residual field is on the order of 0.5 mG. The rf field is produced by a 3-cm long wire parallel to the atomic beam, thus limiting the transit-time broadening contribution to the width of the rf transitions to ~10 kHz for thermal atomic beams.

The laser used was a Coherent-Radiation model 599 cw dye laser actively stabilized on a reference cavity. The linewidth was ~2 MHz; the continuous tuning range 30 GHz. The laser wavelength was initially set using a 0.5-m monochromator and for higher resolution, continuously monitored with 75- and 1.5-GHz interferometers. A stable 300-MHz confocal Fabry-Perot was used to produce markers to calibrate the laser frequency scan. This calibration was subsequently refined by using the measured rf intervals of the initial levels. The drift of the 300-MHz Fabry-Perot was monitored with a frequency stabilized He-Ne laser.

IV. MEASUREMENTS

A. Laser-induced fluorescence

The classification of the Sm I spectrum has been based primarily on infrared spectra.[7] Observed visible transitions have been published by Meggers *et al.*[12] The incomplete nature of these visible-wavelength observations was established immedi-

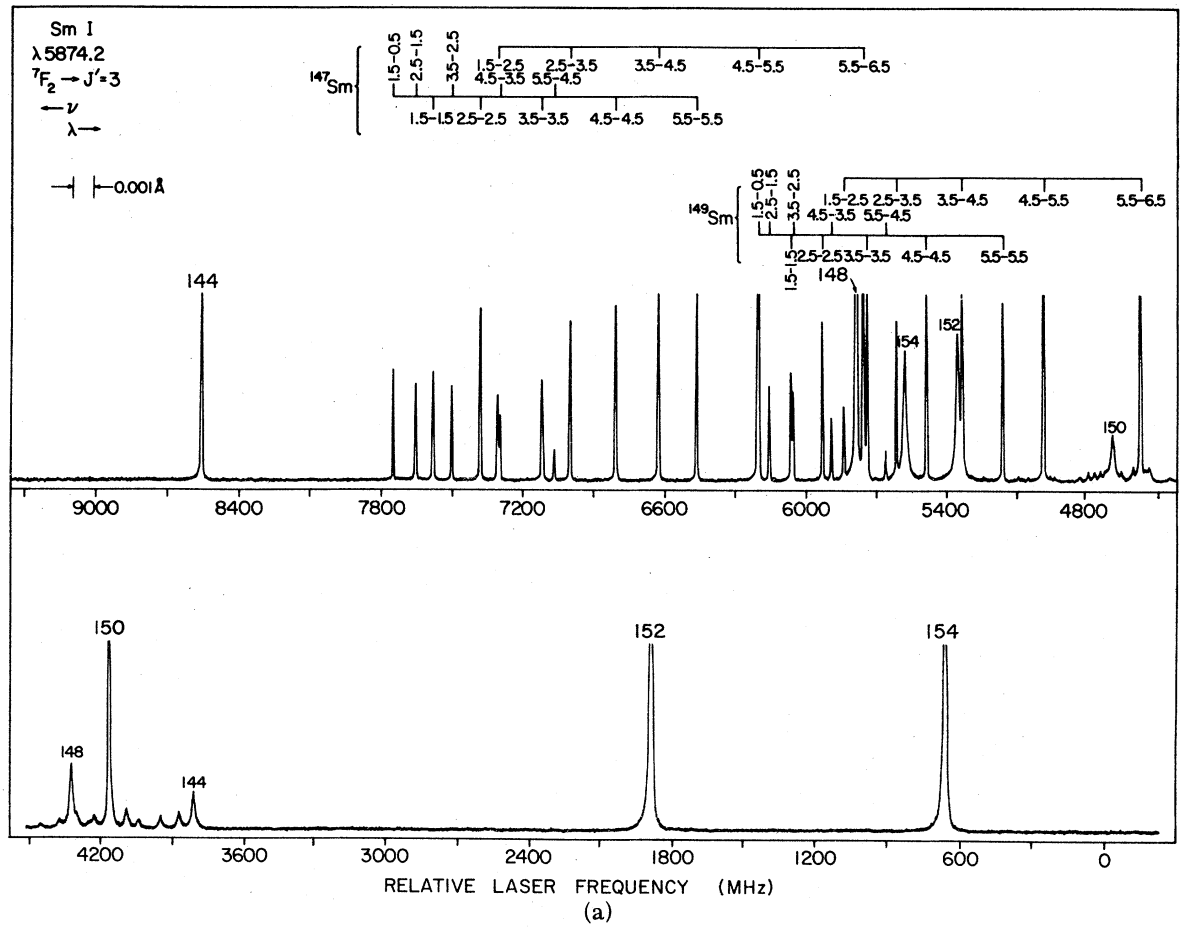

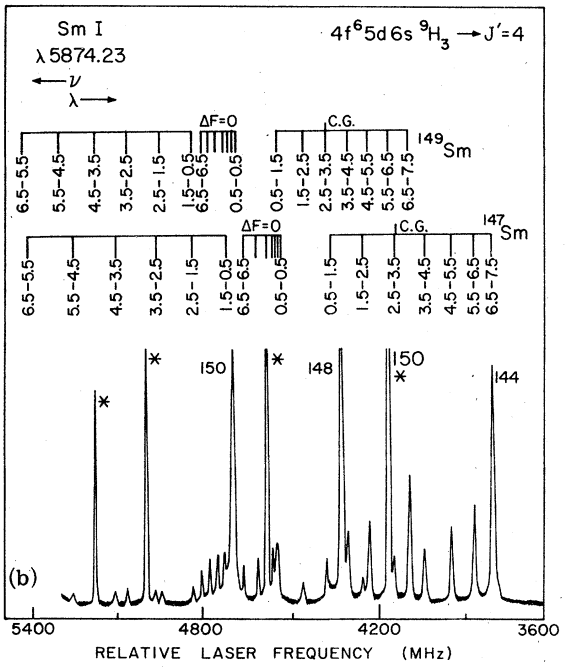

FIG. 2. Part of laser scan around λ_{air} 5874.2 Å, showing (a) the $f^6s^2\,^7F_2 \rightarrow J' = 3$ transition at 5874.21 Å as well as a weaker, strongly overlapping feature. When the discharge was optimized, this feature was identified completely (b) as the $f^6ds\,^9H_3 \rightarrow (f^6dp + f^5d^2s)^7H_4^o$ transition at 5874.23 Å. In both (a) and (b), the contributions of the even-mass isotopes to the $J=2 \rightarrow 3$ transition are denoted by mass numbers in large type, and those to the $J=3 \rightarrow 4$ transition by smaller type numbers. In (b), asterisks are used to indicate components that arise from the $J=2 \rightarrow 3$ transition. In both figures, the F values for the lower and upper levels are indicated for each component above the spectra.

ately with the high resolution of the laser-induced fluorescence technique. Tuning the dye laser in the region around 5874.21 Å, to observe the line from the $^7F_2$ member of the $4f^6 6s^2$ ground multiplet to a $J'=3$ level at 17830.80 cm^{-1}, several lines were observed even though no other transitions had been reported within ±1 Å (Ref. 12) from it. Figure 2(a) illustrates this situation. The $^7F_2 \rightarrow J'=3$ transition is clearly seen together with another transition which is easily identified using the energy level classification of Blaise *et al.*[7] to be a $J=3 \rightarrow J'=4$ transition (11 406.5 $cm^{-1} \rightarrow$ 28 925.30 cm^{-1}). The contribution of the even-A Sm isotopes to the spectrum are indicated by mass numbers in large type for the $J=2 \rightarrow J'=3$ transition, and by smaller type for the $J=3 \rightarrow J'=4$ transition.

The spectrum was obtained with a single laser scan, with the pump beam blocked and 10^{-3}-W/cm^2 probe-laser power, taken in about 4 min, directly on a strip chart recorder. The 3 → 4 transition is solely discharge populated. The numbers at the top of the figure give the values of F for the initial and final states in the transition. Figure 2(b) shows the 3 → 4 part of the spectrum obtained after optimizing the discharge. The linewidth in the $^7F_2 \rightarrow J'=3$ multiplet is ~5 MHz, which is the instrumental limit. The components of the 3 → 4

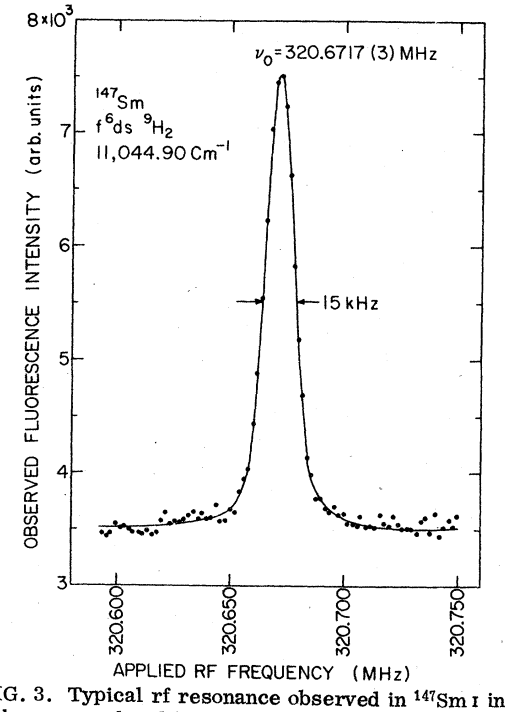

FIG. 3. Typical rf resonance observed in ^{147}Sm I in a discharge-populated level. Recording time was 20 s. The rf level was 0.1 V, which was far below the level needed to give rise to power broadenings or shifts. This was verified experimentally.

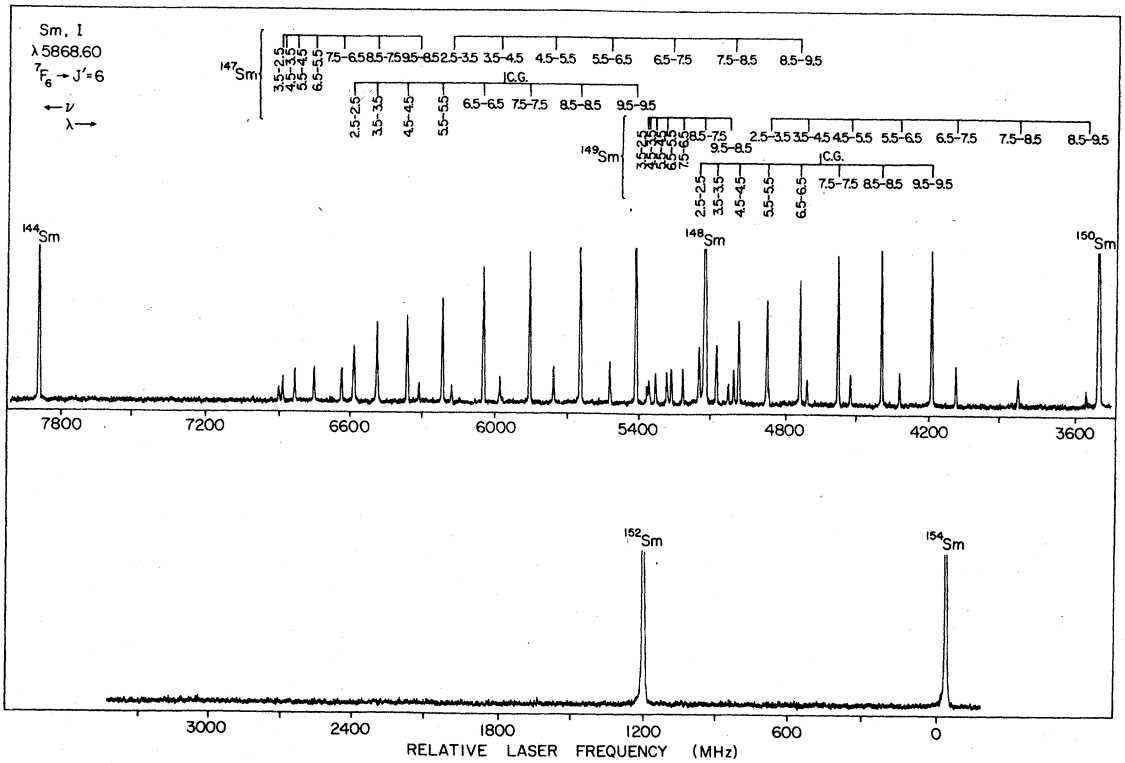

FIG. 4. The $f^6s^2\,{}^7F_6 \rightarrow f^6sp\,{}^7F^o_6$ transition at λ_{air} 5868.60 Å, completely resolved in laser-induced fluorescence. The linewidth of 4 MHz is instrumentally limited. The values of F associated with the lower and upper levels are given for each component above the spectrum.

transition have a linewidth of ~8 MHz, corresponding to a lifetime of 19 ± 3 ns for the $J' = 4$ (28 425.30 cm^{-1}) level. In Fig. 2(b), the four components that arise from the $J = 2 \rightarrow 3$ transition are indicated by asterisks; all others are due to the $J = 3 \rightarrow J' = 4$ transition. It is interesting to note that the IS is of opposite sign for the two transitions. No power broadening is observed at the applied laser intensity, but was clearly observable at powers $\gtrsim 10^{-1}$ W/cm^2.

B. Laser-rf double-resonance spectroscopy

To perform laser-rf double-resonance spectroscopy, spectra like Fig. 2 were completely analyzed for both hfs and IS, to classify and obtain the energy-level splittings in the two odd isotopes ^{147,149}Sm I to better than 1%. In Fig. 2 this classification is indicated. Setting the laser on a particular hfs transition, with the pump beam allowed to intersect the atomic beam, a rf search within 1 MHz easily revealed the resonant frequency by a sharp increase in the fluorescence induced by the probe laser. Figure 3 shows a typical rf resonance. To test the accuracy of this technique the transition from the ground configuration $4f^6 6s^2\,{}^7F_6$ to $f^6 sp\,{}^7F_6^o$ was observed (Fig. 4) by laser-induced fluorescence, making it possible to apply the laser-rf double-resonance technique. In Sec. V the rf results for the $4f^6 6s^2\,{}^7F_6$ level, all obtained in a few hours, are compared to previous high-precision atomic-beam magnetic-resonance experiments[6] performed with great difficulty on a thermally populated atomic beam. Laser-rf double-resonance data for highly excited metastable levels as well as hfs of upper states, deduced from laser-fluorescence spectra, and isotope shift results are also discussed.

V. ANALYSIS AND RESULTS

Because of the extreme richness of the fine-structure spectrum and our lack of a precision means of measuring wavelength, the identification of an observed line as due to a transition between a particular pair of known levels was often difficult. The very large number of components for each line (typically 40–60) usually precluded any identification based on less than a detailed analysis of all the components.

Identification of each line was normally achieved by assuming values of J and J' (the J values of the lower and upper states, respectively) and then carefully comparing the observed relative intensities with the calculated values. For a given identification of the components, least-squares fits of the magnetic-dipole hfs constants A and electric-quadrupole constants B of the upper and lower states to the observed spectrum were made. Once the correct identification of the components had been found, the fit was always of high quality. For these fits, the ratios $A(^{147}\mathrm{Sm})/A(^{149}\mathrm{Sm})$ and $B(^{147}\mathrm{Sm})/B(^{149}\mathrm{Sm})$ were held equal to the ratios previously determined by radio-frequency measurements[6] in the ground multiplet $4f^6 6s^2\,{}^7F_{1-6}$.

Analysis of the radio-frequency, double-resonance data was somewhat more straightforward than for the optical spectra. The standard expressions for the hyperfine splittings of a level were fitted to the observed $\Delta F = \pm 1$ intervals by varying A and B for the lower state. Inclusion of a magnetic-octopole hfs interaction constant C yielded very small values of C (several hundred Hz or smaller) as expected for the nonpenetrating $4f$ electrons. Furthermore, it is well known that inclusion of magnetic-octopole or electric-hexadecapole interactions is meaningless unless the shifts of the hyperfine levels due to second-order hyperfine interactions with neighboring atomic states are carefully taken into account. Although these effects could in principle be included in the analysis, detailed knowledge of the eigenvectors of all perturbing states up to and beyond 30 000 cm^{-1} would be needed. The data presented here do not include these very small corrections.

The hfs constants of the $4f^6 6s^2\,{}^7F_6$ level were redetermined by measuring all hyperfine intervals in both ^{147}Sm and ^{149}Sm. The observed intervals, and the results of the least-squares, two-parameter fit to each isotope are given in Table I. It is seen that the self-consistency, even without including the second-order corrections and the octopole and hexadecapole interaction constants

TABLE I. Observed and calculated hfs intervals in the $f^6 s^2\,{}^7F_6$ level. The observed frequencies are not corrected for off-diagonal hfs interactions. Taking them into account improves the fit and yields nuclear moment ratios equal to those of the other J members of the $f^6 s^2\,{}^7F$ multiplet.

A	$F \leftrightarrow F'$	ν_{obs} (MHz)	ν_{calc} (MHz)	obs. − calc. (kHz)
147	9.5–8.5	675.4092	675.4123	−3.1
	8.5–7.5	637.9913	637.9887	2.6
	7.5–6.5	589.3404	589.3372	3.2
	6.5–5.5	530.7844	530.7878	−3.4
	5.5–4.5	463.6533	463.6531	0.2
	4.5–3.5	389.2553	389.2528	2.5
	3.5–2.5	308.9162	308.9178	−1.6
149	9.5–8.5	633.6144	633.6134	1.0
	8.5–7.5	557.1804	557.1789	1.5
	7.5–6.5	483.9897	483.9916	−1.9
	6.5–5.5	413.666	413.6672	−1.2
	5.5–4.5	345.825	345.8250	0.0
	4.5–3.5	280.083	280.0845	−1.5
	3.5–2.5	216.062	216.0603	1.7

C and D, is within ±4 kHz. This level of precision is substantially higher than that achieved earlier[6] by the atomic-beam magnetic-resonance technique, but is in good agreement with the earlier work.

This level of self-consistency is also found in the rf measurements on the discharge-populated states. All of the hyperfine-structure results are summarized in Table II. The first four lines of the table give the high-precision results measured by the laser-rf double-resonance technique and the last six lines give results of much lower precision achieved simply by interpretation of the fluorescence spectra. For each measurement based only on optical data, however, the frequency scale was calibrated by many-lower-state hfs intervals precisely measured by rf techniques.

The ratios $(^{147}A/^{149}A)$ and $(^{147}B/^{149}B)$ with A, B values corrected for off-diagonal hyperfine interactions has been obtained earlier by atomic-beam magnetic-resonance[6] for the ground f^6s^2 term. The new improved values of the hyperfine intervals in the $f^6s^2\,^7F_6$ level, obtained in this work, corrected for off-diagonal hyperfine interactions[6] are consistent within the uncertainty limits with the average values of $(^{147}A/^{149}A)$ and $(^{147}B/^{149}B)$ for the first five states of $f^6s^2\,^7F_J$.

The ratios for the $f^6ds\,^7H_3$ level at 13 542.80 cm^{-1}, not corrected for any off-diagonal hyperfine interactions, are very closely equal to the ratio for the ground multiplet for $(^{147}A/^{149}A)$ indicating that such second-order effects are very small; the $(^{147}B/^{149}B)$ ratio is also close to the equivalent ground-configuration ratio, again indicating small admixtures due to off-diagonal hfs interaction.

This is not the case for the $f^6ds\,^9H_2$, $^9H_3$ levels at 11 044.90 cm^{-1} and 11 406.50 cm^{-1}, respectively, where the ratios differ from the corrected values for the ground ^7F term by about 20 times the uncertainty limits. As no eigenvectors exist for these excited states, off-diagonal hfs corrections can not be applied, but these results clearly indicate that they are substantial, most probably due to the presence of perturbing levels near this excitation energy.

In addition to the effects of second-order hfs, there is evidence of strong spin-orbit mixing for the $^9H_{2,3}$ states. It is straightforward to show, for example, that the B factor for a pure $f^6ds\,^9H_2$ level is zero, including all relativistic contributions, while the observed value (for ^{147}Sm) is ~ -11.7 MHz. In addition, the value observed for the $^9H_3$ level B (^{147}Sm, $^9H_3$) ≈ -20.8 MHz is much larger than the value −2 MHz one would estimate for a pure $f^6ds\,^9H_3$ state. Much less can be said about the A values, however, since the *two* measured A values (for $^9H_{2,3}$) both depend on the hfs contributions of the *three* electron shells $4f$, $5d$, and $6s$. Nevertheless, when reasonable values are chosen for these contributions, the lack of consistency with the data again indicates strong admixture for the $^9H_{2,3}$ levels. It is planned to extend the present high-precision measurements to additional levels, and to make a systematic analysis of the results.

Isotope shifts were determined not only for the lines listed in Table II, but also for a number of other lines. No effort was made to achieve very high precision for the IS measurements. Because the components arising from three of the five even-A isotopes (^{154}Sm, ^{152}Sm, and ^{144}Sm) lie well outside of the hfs patterns of the odd-A isotopes for virtually every line, the precisely known

TABLE II. Experimentally measured hfs interaction constants. The first four lines give laser-rf double-resonance data not corrected for any off-diagonal hfs interaction, whereas the rest are deduced from laser-induced fluorescence spectra. The $f^6sp\,^7F_1^o$ level has previously been measured (Ref. 4) in agreement with this work.

Level	Energy (cm^{-1})	λ_{obs}^{air} (Å)	^{147}A (MHz)	^{149}A (MHz)	^{147}B (MHz)	^{149}B (MHz)
$f^6s^2\,^7F_6$	4 020.66	5868.60	−78.3585(4)	−64.5958(4)	203.3501(20)	−58.8107(20)
$f^6ds\,^9H_2$	11 044.90	5898.96	−92.8699(4)	−76.5683(4)	−11.6586(20)	3.2192(20)
$f^6ds\,^9H_3$	11 406.50	5874.23	−122.1573(4)	−100.6514(4)	−20.8263(20)	5.9040(20)
$f^6ds\,^7H_3$	13 542.80	5875.08	−101.4747(7)	−83.6516(4)	17.7920(40)	−5.2276(20)
$f^6sp\,^7F_1^o$	17 769.71	5895.34	−394.9(10)	−325.5(10)	−20.4(50)	5.9(50)
$f^6sp\,^5G_3^o$	17 830.80	5874.21	−110.3(10)	−90.9(10)	−10(7)	3(7)
$f^6sp\,^7F_6^o$	21 055.76	5868.60	−104.0(10)	−85.8(10)	248.4(50)	−72.7(50)
$J'=3$	27 992.35	5898.96	−101.8(10)	−83.9(10)	−4.6(8)	1.3(8)
$(f^6dp+f^5d^2s)\,^7H_4^o$	28 425.30	5874.23	−116.3(10)	−95.9(10)	18.6(60)	−5.3(60)
$J'=3$	30 559.13	5875.08	−176.2(10)	−145.3(10)	13.9(7)	−4.0(7)

spacings between hfs components could not be used to determine the isotope shifts. The shifts were therefore determined primarily from the 300-MHz markers, but these were subject to a small systematic error due to thermal drifts ($\lesssim 10$ MHz) in the étalin during a laser scan.

The isotope shifts involving the odd-A isotopes were evaluated easily once the hfs components had been identified and the center of gravity of the pattern determined by application of the elementary hfs theory.

A convenient way of summarizing the isotope-shift results is to display them in a King plot.[13] To do this, the modified isotope shifts[14,15] are calculated by multiplying the observed shifts by $A_1A_2/(A_2-A_1)$ to take account of the $1/A^2$ dependence of the mass effect; A_1 and A_2 are the mass numbers of the isotopes involved. When the modified shift is then plotted against that for a reference line, a straight line must result if the standard theory of the isotope shift is correct.[15] Figure 5 shows the present results. The transition λ5874.21 from $4f^6 6s^2\,{}^7F_2$ (811.92 cm^{-1}) $\rightarrow J'=3$ (17830.80 cm^{-1}) was chosen as the reference line. In order to keep the units convenient, all of the modified shifts were divided by $154\times152/(154-152)$ before plotting; this equivalent to selecting the isotope pair (154, 152) as a standard.

It can be seen in Fig. 5 that the points do indeed fall on straight lines as required by the elementary theory. No anomalies are found for the odd-A isotopes in spite of the severe odd-even staggering in the isotope shifts. This finding is in agreement with the recent high-precision work of Brand *et al.*[4]

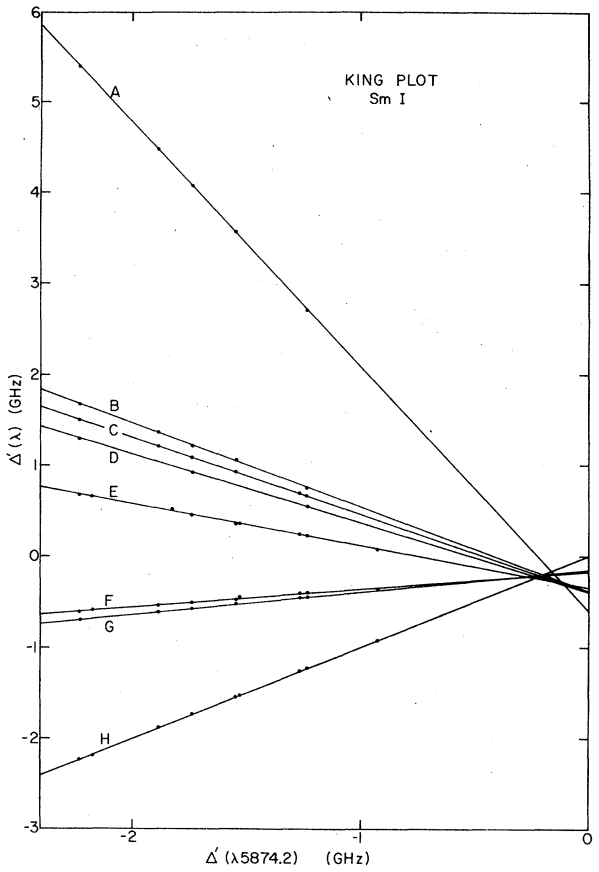

FIG. 5. King plot of all observed transitions. All reduced isotope shifts are plotted against λ5874.21 ($J=2\rightarrow3$), ^{152,154}Sm being taken as the reference pair. (A) Not identified, λ_{air} 5875.1 Å; (B) 292.58 cm$^{-1}\rightarrow$17810.85 cm^{-1}; (C) 14563.98 cm$^{-1}\rightarrow$31597.53 cm^{-1}; (D) 16392.93 cm$^{-1}\rightarrow$33408.80 cm^{-1}; (E) 11044.90 cm$^{-1}\rightarrow$27992.35 cm^{-1}, 13542. 80 cm$^{-1}\rightarrow$30559.13 cm^{-1}, and 11406.50 cm$^{-1}\rightarrow$28425.30 cm^{-1}, all with virtually identical King plot; (F) 811.92 cm$^{-1}\rightarrow$17769.71 cm^{-1}; (G) 2273.09 cm$^{-1}\rightarrow$19210.09 cm^{-1}; (H) 4020.66 cm$^{-1}\rightarrow$21055.76 cm^{-1}. The energies refer to Blaise *et al.*[7] Since line (A) cannot be identified from any of the levels given by Blaise *et al.*, the lower level in the transition is presumed to lie higher than 18160 cm^{-1}.

VI. CONCLUSIONS

The laser-rf double-resonance technique may be compared with high-precision, Doppler-free laser spectroscopy and with the traditional atomic-beam magnetic-resonance techniques as tools for obtaining precision hfs data. The double-resonance scheme easily gives a precision about 2000 times better than that from the best *commercial* dye laser systems. The rf-laser technique appears to enjoy most of the advantages of the conventional atomic-beam magnetic-resonance technique, but it is likely to be substantially more precise for the same rf arrangement because (a) there is no uncertainty in the magnetic field (a small field broadens the line symmetrically rather than shifts it), and (b) all the hyperfine intervals can be measured instead of just those involving the large F values, since the observability of a given transition is not dependent on the restrictive selection rules of magnetic-deflection machines.

ACKNOWLEDGMENTS

One of the authors (O.P.) acknowledges partial support from the Danish Natural Science Research Council. Work was performed under the auspices of the Division of Basic Energy Sciences of the Dept. of Energy.

*Permanent address: Institute of Physics, University of Aarhus, DK8000 Aarhus C, Denmark.

[1]A. R. Striganov, V. A. Katulin, and V. V. Eliseev, Opt. Spectrosc. 12, 91 (1962).
[2]W. H. King, J. Opt. Soc. Am. 53, 638 (1963).
[3]J. E. Hansen, A. Steudel, and H. Walther, Z. Phys. 203, 296 (1967).
[4]H. Brand, B. Nottbeck, H. H. Schulz, and A. Steudel, J. Phys. B 11, L99 (1978).
[5]J. Bauche, R. J. Champeau, and C. Sallot, J. Phys. B 10, 2049 (1977).
[6]G. K. Woodgate, Proc. R. Soc. London Ser. A 293, 117 (1966); R. G. H. Robertson, J. C. Waddington, and R. G. Summers-Gill, Can. J. Phys. 46, 2499 (1968); W. J. Childs and L. S. Goodman, Phys. Rev. A 6, 2011 (1972).
[7]J. Blaise, C. Morillon, M. G. Schweighofer, and J. Verges, Spectrochim. Acta Part B 24, 177 (1969).
[8]S. D. Rosner, R. A. Holt, and T. D. Gaily, Phys. Rev. Lett. 35, 785 (1975).
[9]W. Ertmer and B. Hofer, Z. Phys. A 276, 9 (1976).
[10]S. D. Rosner, T. D. Gaily, and R. A. Holt, Phys. Rev. Lett. 40, 851 (1978).
[11]M. Dubke, W. Jitschin, G. Meisel, and W. J. Childs, Phys. Lett. A 65, 109 (1978).
[12]W. F. Meggers, C. H. Corliss, and B. F. Scribner, *Tables of Spectral-Line Intensities*, Part 1, Natl. Bur. Stand. Monograph 145 (U.S. GPO, Washington, D.C., 1975).
[13]W. H. King, J. Opt. Soc. Am. 53, 638 (1963).
[14]J. E. Hansen, A. Steudel, and H. Walther, Phys. Lett. 19, 565 (1965).
[15]K. Heilig and A. Steudel, At. Data Nucl. Data Tables 14, 613 (1974).